LETTER TO THE EDITOR

Molecular basis for histidine N1 position-specific methylation by CARNMT1

Cell Research (2018) 28:494–496; https://doi.org/10.1038/s41422-018-0003-0

Dear Editor,

Methylation often serves as a biochemical strategy to add new traits of the modified residue for recognition and regulation. Besides arginine and lysine methylations, histidine can also undergo methylation in proteins or histidyl peptides, such as ribosome protein Rpl3, actin,[1,2] and dipeptide carnosine (β-alanyl-L-histidine).[3] The methylation can occur on either N1 or N3 position of the histidine imidazole ring, and such a position specificity is catalyzed by different histidine methyltransferases (Fig. 1a).[1] For instance, yeast YIL110W methylates histidine 243 at the N3 position of yeast Rpl3, which promotes 60S ribosome subunit assembly and the fidelity of translational elongation.[4,5] The enzyme CARNMT1 (carnosine N-methyltransferase 1, also known as C9orf41), conserved from yeast to human, was identified as an N1 position-specific methyltransferase that catalyzes the conversion of carnosine to anserine (β-alanyl-N-π-methyl-L-histidine) (Fig. 1a).[6] The N1- or N3-specific histidine methylation underscores a position-specific layer of regulation, reminiscent of state-specific methylation of lysine or arginine residues in histones.[7] However, due to lack of structural information, the molecular basis underlying substrate recognition and position-specific catalysis remains largely unexplored.

To this end, we first determined the binary crystal structure of human CARNMT1 (aa 53–409) bound to methyl donor S-(5′-Adenosyl)-L-methionine (SAM) at 2.25 Å (Supplementary information, Table S1). CARNMT1 adopts a canonical SAM-MTase (SAM-dependent methyltransferase) core fold consisting of a seven-stranded β sheet (β1-β7) adjoined by six flanking α helices (α1-α6) (Fig. 1b). The SAM cofactor binds to a central cleft formed by the topological switch-point elements next to β1 (Fig. 1c). The SAM binding site is characteristic of a "GxGxG" (G_{208}-A_{209}-G_{210}-L_{209}-G_{212}) nucleotide-binding motif linking β1 and α2 (Supplementary information, Figure S1A); and SAM forms extensive hydrogen bonding interactions with surrounding residues that are structurally conserved between yeast and human (Supplementary information, Figure S1B).[8] The enzyme also has several additional structural elements, including four helices (αA, αB, αC and αD) from the N-terminus and an extended β hairpin (β1′, β2′ and αE) inserted between β2 and β3 within the core domain (Fig. 1b, c). These additional structural elements are often divergent among SAM-MTase family members and usually account for the methylation substrate specificity. Structural and SEC-MALS (size exclusion chromatography followed by multi-angle light scattering) analyses revealed that CARNMT1 functions as a symmetric dimer (Supplementary information, Figure S1C and D). The dimer is notably stabilized by anti-parallel β sheet (β7/β7′) formation around the symmetry center and helix bundle contacts among α6 and αA′-αB′-αC′.

Next, we determined the ternary complex structure of CARNMT1 bound to carnosine and Sinefungin (SFG, a SAM analog) at 2.4 Å (Supplementary information, Table S1). Crystal structure revealed positioning of two copies of carnosine and SFG within one CARNMT1 dimer (Fig. 1d). Each copy of carnosine and SFG is accommodated in a central cleft of each monomer, with carnosine located next to the symmetry center. The two carnosine molecules are interleaved by a pair of symmetry-related tyrosine residues (Y396) at the dimer interface (Fig. 1d). Upon carnosine binding, the two Y396 residues take on asymmetric conformations and become partially disordered (Supplementary information, Figure S2A), suggesting a mechanism of substrate cross-talk through the route of "carnosine-Y396-Y396′-carnosine" in the context of CARNMT1 dimer. The impact of such a cross-talk on enzymatic activity awaits further kinetic studies.

As shown in Fig. 1e, carnosine is docked into a pocket formed by loops L4, α5′, L5, L67, β7 and αD. Superimposition of carnosine-bound ternary structure and SAM-bound binary structure revealed induced side-chain rotamer change of H347 and Y396 (Supplementary information, Figure S2B). Carnosine is deeply buried in the active pocket formed by residues F313, D316, P343, L345, H347, Y386, Y396 and Y398 (Fig. 1f). In addition to hydrophobic contacts contributed by F313, P343, L345 and Y386, two pairs of hydrogen bonds involving residues D316 and Y398, as well as cation-π interaction between the N-terminal amine of carnosine and Y396 phenol ring define the orientation of carnosine. Notably, D316 is directly hydrogen bonded to N3 of histidine, which determines a flipping orientation of the imidazole ring so that N1 is present next to SAM (represented by SFG) for methylation (Fig. 1f). Owing to its negative charge, D316 can also serve as a catalytic residue by facilitating the deprotonation of N1 to initialize the nucleophilic attack in an S_N2-like methyl transfer reaction.[9]

We also solved the ternary structure of CARNMT1 bound to anserine and SAH at 2.8 Å (Supplementary information, Table S1). As evidenced by the omit electron density map, we were able to capture two states of the histidine methylation cycle: the pre-methyl transfer state that is represented by the CARNMT1-carnosine-SFG complex (Fig. 1g(i)) and the post-methyl transfer state that is represented by the CARNMT1-anserine-SAH complex (Fig. 1g(ii)). Alignment among three aforementioned structures revealed a ~90° side-chain rotation of H347 in the carnosine-SFG bound ternary complex (Fig. 1h). The flipped H347 is stabilized by two sets of hydrogen bonding interactions involving the main-chain carbonyl of L345 and a water molecule that is further hydrogen bonded to the δ-amine of SFG and conceivably the δ-methyl of SAM. Notably, H347 stacks against the imidazole ring of carnosine in an "edge to face" fashion. We measured a distance of ~3.6 Å between the C2 atom of H347 and the imidazole ring, supporting the existence of "methyl-π" interaction.[10] In the post-methyl transfer state of the anserine-SAH complex, H347 flips back to its substrate-free state, which suggests a "hold-release" switching role of H347 for the benefit of substrate binding and product release. Moreover, the flipping of H347 creates a snug

Received: 10 October 2017 Revised: 7 December 2017 Accepted: 12 December 2017
Published online: 20 February 2018

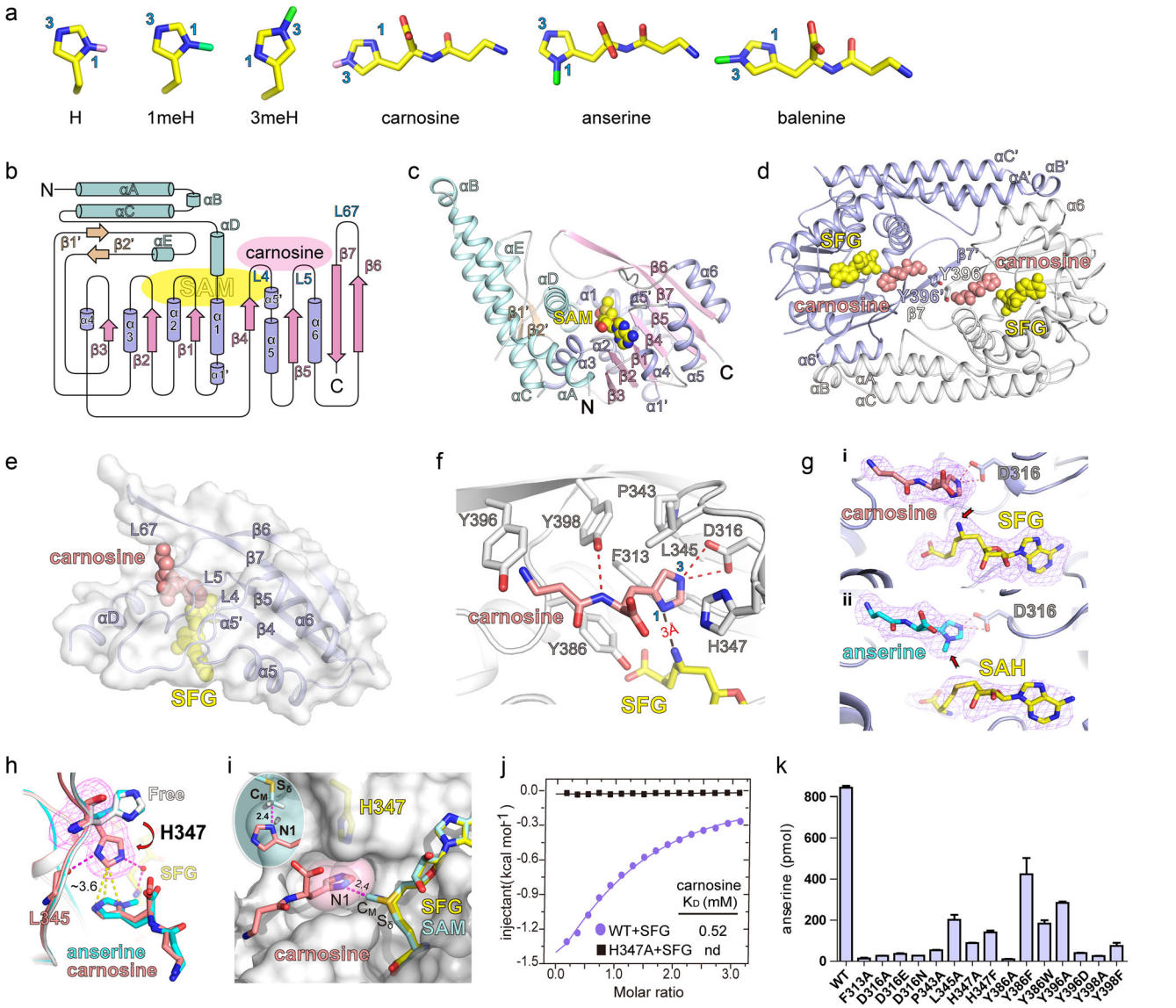

Fig. 1 Molecular basis for histidine N1 position-specific methylation by CARNMT1. **a** Chemical structures of histidine (H), N1-methylated histidine (1meH), N3-methylated histidine (3meH), carnosine, anserine (N1-methylated carnosine), and balenine (N3-methylated carnosine). Carbon, nitrogen, hydrogen and methyl are shown as yellow, blue, pink and green sticks, respectively. For clarity, main chains of H, 1meH and 3meH are omitted from representation. **b** Topology of CARNMT1 catalytic domain. The canonical SAM-MTase core fold is shaded blue (α helices) and pink (β strands), respectively. The additional elements are colored palegreen (α helices) and wheat (β strands), respectively. Carnosine- and SAM-binding motifs are shaded pink and yellow, respectively. **c** Overall structure of CARNMT1 monomer in ribbon view. The color coding is the same as in **b**. **d** Overall structure of CARNMT1 dimer bound to carnosine and SFG. Carnosine and SFG are depicted as spheres and colored pink and yellow, respectively. A pair of Y396 residues are shown as sticks. Key secondary elements participating in dimer formation are labeled. **e** Positioning of carnosine in the binding pocket of a CARNMT1 monomer. The secondary structural elements constituting the carnosine pocket includes αD, L4, L5, α5′ and L67. **f** Interaction details within the carnosine pocket. Key residues that participate in carnosine binding are depicted as white sticks. **g** The Fo-Fc omit map of carnosine and SFG (panel i), anserine and SAH (panel ii) contoured at 2.0 σ level. D316 is shown as sticks. **h** Side-chain flipping of H347 among CARNMT1-SAM (white), CARNMT1-carnosine-SFG (pink), and CARNMT1-anserine-SAH (cyan). The Fo-Fc omit map of H347 in the CARNMT1-carnosine-SFG ternary complex is contoured at 3.0 σ level. Small red ball, water. **i** Burial of the carnosine imidazole ring in a narrow pocket created by the flipped H347. Cofactor SAM is modeled by structural superimposition over SFG. The "in-line" geometry of the active center is highlighted in the close-up panel. **j** Calorimetric titration fitting curves of wild-type (WT) and mutant CARNMT1 titrated with carnosine in the presence of SFG. nd, not detected. **k** In vitro methyltransferase assay of WT and annotated CARNMT1 mutants. Enzymatic activity was monitored by the yield of anserine in the unit of pmol converted from 10 nmol carnosine by 250 pmol CARNMT1 in 1 h as quantified by LC-MS

pocket that nicely grips and consequently constrains the imidazole ring of carnosine, leaving only N1 available for methylation. To analyze the active site geometry for catalysis, we modeled the SAM cofactor into the carnosine-SFG complex by structural alignment of SAM in the binary complex over SFG in the ternary complex. We measured a distance of 2.4 Å between N1 and the carbon of δ-methyl (C_M), and a vector angle of ~40° between the lone pair of electrons on the N1 and $S_δ$-C_M (Fig. 1i). Such an approximate "in-line" geometry of the reactant complex is well consistent with an active site structure for S_N2-like methyl transfer reaction investigated in previous computational chemistry studies.[9]

To explore the role of H347 in substrate binding, we performed isothermal calorimetric titrations using wild-type and H347A

mutant samples titrated with carnosine (Fig. 1j). In the presence of SFG, we measured a binding K_D of 0.52 mM for wild-type CARNMT1, whereas the binding was not detectable for H347A, highlighting the critical contribution of H347 in substrate recognition. To determine the functional importance of key residues constituting the carnosine pocket, we generated CARNMT1 mutants including F313A, D316A, D316E, D316N, P343A, L345A, H347A, H347F, Y386A, Y386F, Y386W, Y396A, Y396D, Y398A and Y398F and performed in vitro methylation assays by LC-MS (Fig. 1k). As expected, the enzymatic activities of these CARNMT1 mutants were either compromised or disrupted. In particular, mutating D316 to glutamate, alanine or asparagine almost completely disrupted enzymatic activities, suggesting that proper size and a negative charge of D316 are essential for both substrate recognition and catalysis (e.g., as a deprotonation base). More than 80% activity loss of H347A and H347F further supports the role of H347 in substrate binding and likely catalysis (e.g., by stabilizing the transition state through water-mediated hydrogen bonding with C_M). The dramatic activity loss of Y398A and Y398F underscores the contribution of phenol hydroxyl-mediated hydrogen bonding interaction for substrate recognition. Moreover, the nearly complete activity loss of F313A and Y386A, stresses the role of these bulky and hydrophobic residues in shaping the base of the carnosine pocket (Fig. 1f).

In summary, here we solved the cofactor-bound binary, substrate- and product-bound ternary crystal structures of human CARNMT1. Our structural studies revealed the substrate binding mode of carnosine, in which N1 position specificity is achieved by precise anchoring of the histidine imidazole ring in a recognition pocket such that N1 but not N3 is exposed and deprotonated for methylation. The exquisite molecular design of N1 versus N3 position specificity of CARNMT1 expands our knowledge on methylation biology and calls attention to a yet to be fully appreciated role of histidine methylation in biological recognition and regulation.

ACCESSION CODES

The atomic coordinates of $CARNMT1_{53-409}$ bound to SAM, carnosine-SFG, and anserine-SAH have been deposited into the Protein Data Bank under accession codes 5YF0, 5YF1, 5YF2, respectively.

ACKNOWLEDGEMENTS

We sincerely thank Dr Jiahuai Han (Xiamen University) for sharing CARNMT1 cDNA. We thank the staff members at beamline BL17U1 of the Shanghai Synchrotron Radiation Facility and Dr S Fan at Tsinghua Advanced Innovation Center for Structural Biology for their assistance with data collection, and the China National Center for Protein Sciences Beijing for providing facility support. This work was supported by the National Key R&D Program of China (2016YFA0500700) and the National Natural Science Foundation of China (91753203 and 31725014) to HL. We also acknowledge Beijing Natural Science Foundation (5182014), Beijing Metropois for the Beijing Novo Program (XX2018046), and China Association for Science and Technology for the Young Elite Scientists Sponsorship Program to YL.

ADDITIONAL INFORMATION

Supplementary information accompanies this paper at https://doi.org/10.1038/s41422-018-0003-0.

Competing Interests: The authors declare no competing financial interests.

Ruili Cao[1], Xingrun Zhang[1], Xiaohui Liu[2], Yuanyuan Li[1] and Haitao Li[1]

[1]MOE Key Laboratory of Protein Sciences, Beijing Advanced Innovation Center for Structural Biology, Tsinghua-Peking Joint Center for Life Sciences, Department of Basic Medical Sciences, School of Medicine, Tsinghua University, Beijing 100084, China and [2]Lipidomics and Metabolomics Centre, National Protein Science Facility, School of Life Sciences, Tsinghua University, Beijing 100084, China

Correspondence: Haitao Li (lht@tsinghua.edu.cn)

REFERENCES

1. Webb, K. J. et al. A novel 3-methylhistidine modification of yeast ribosomal protein Rpl3 is dependent upon the YIL110W methyltransferase. *J. Biol. Chem.* **285**, 37598–37606 (2010).
2. Elzinga, M. Amino Acid Sequence around 3-Methylhistidine. *Biochemistry* **10**, 224–229 (1971).
3. Mcmanus, I. R. Enzymatic Synthesis of Anserine in Skeletal Muscle. *J. Biol. Chem.* **237**, 1207–1211 (1962).
4. Al-Hadid, Q. et al. Histidine methylation of yeast ribosomal protein Rpl3p is required for proper 60S subunit assembly. *Mol. Cell. Biol.* **34**, 2903–2916 (2014).
5. Al-Hadid, Q. et al. Methylation of yeast ribosomal protein Rpl3 promotes translational elongation fidelity. *RNA* **22**, 489–498 (2016).
6. Drozak, J. et al. UPF0586 Protein C9orf41 Homolog Is Anserine-producing Methyltransferase. *J. Biol. Chem.* **290**, 17190–17205 (2015).
7. Taverna, S. D. et al. How chromatin-binding modules interpret histone modifications: lessons from professional pocket pickers. *Nat. Struct. Mol. Biol.* **14**, 1025–1040 (2007).
8. Liu, X. et al. Substrate Recognition Mechanism of the Putative Yeast Carnosine N-methyltransferase. *ACS Chem. Biol.* **12**, 2164–2171 (2017).
9. Guo, H. B. & Guo, H. Mechanism of histone methylation catalyzed by protein lysine methyltransferase SET7/9 and origin of product specificity. *Proc. Natl Acad. Sci. USA* **104**, 8797–8802 (2007).
10. Liao, S. M. et al. The multiple roles of histidine in protein interactions. *Chem. Cent. J.* **7**, 44 (2013).